ISBN: 978-3-95450-248-6 ISSN: 2673-5490 doi: 10.18429/JACoW-IPAC2025-WEPM061

DYNAMIC APERTURE MODELS FOR A TIME-VARYING HIGH LUMINOSITY LHC LATTICE*

C.E. Montanari[1], M. Giovannozzi, G. Sterbini, CERN, Geneva, Switzerland
R.B. Appleby, University of Manchester, Manchester, United Kingdom
[1]also at University of Manchester, Manchester, United Kingdom

Abstract

The evaluation of dynamic aperture (DA) under time-dependent variations of lattice parameters is essential for understanding the long-term stability of particle motion in the Large Hadron Collider (LHC) and enhancing the future performance of the High-Luminosity LHC (HL-LHC). In this work, we develop DA models that address the complexities introduced by time-varying effects, with a focus on the operational challenges posed by luminosity levelling. Building on established DA scaling laws, we aim at capturing the impact of evolving machine conditions during levelling. An initial simulation study is presented that compares the effects on DA of different levelling schemes that are expected to be routinely used during the HL-LHC operation, providing key insight into extending current DA models to accommodate time-dependent perturbations.

INTRODUCTION

HL-LHC [1] is a major upgrade initiative aimed at significantly increasing the integrated luminosity delivered to the ATLAS and CMS experiments at the LHC [2]. Achieving this ambitious luminosity goal relies on several technological and operational advancements. These include higher beam intensities and improved beam brightness, made possible by the LHC Injectors Upgrade (LIU) [3]. Another key development is the use of advanced optics schemes, such as the Achromatic Telescopic Squeeze (ATS) [4], which provides enhanced control over chromatic effects at the lowest values of β^* at the high-luminosity interaction points (IPs). Additionally, new components such as crab cavities [5] will mitigate luminosity losses caused by the large crossing angles required to mitigate strong beam-beam effects.

A critical factor influencing the success of HL-LHC operations is the dynamic aperture (DA) [6], a key parameter that quantifies the extent of the stability region in the phase space within which particle trajectories remain bounded for a certain number of turns. Maintaining an adequate DA is essential to ensure an acceptable beam lifetime [7] and containing beam losses. Traditionally, DA is evaluated under static lattice configurations [8, 9], providing limited information on the effects of changing operational conditions. In particular, established DA scaling laws have also been constructed and validated under these static conditions [10, 11], raising important questions about whether these scaling laws require modifications to account for time-dependent accelerator lattices. In this paper, we study a novel DA tracking method in which multiple time-varying lattice elements are simultaneously considered, and we present an assessment of how these dynamic conditions impact both the DA and established scaling laws, providing insights into beam stability under complex, time-dependent lattice manipulations.

TIME-VARYING LATTICES FOR DYNAMIC APERTURE SIMULATIONS

Generalities

We examine a series of HL-LHC lattices for which beam-beam effects on DA was studied [12]. As in this previous analysis, we perform simulations using Xsuite [13, 14] for both optics matching and multi-turn tracking. Beam-beam effects are simulated using the weak-strong approach [15]. Compared to the previous study, which defined DA as the minimum stable radial amplitude over a radial grid (5 angles, 0.03 σ radial step), we adopt the definition based on the angular average over a denser grid with 25 angles and a 0.05 σ radial step in the x–y plane [6]. This refined sampling approach provides a more reliable DA estimate, especially in the presence of time-dependent lattice perturbations, and is expected to yield a statistical uncertainty of 0.05 σ in DA evaluations, following the approach in [10].

The HL-LHC configuration used corresponds to the layout version 1.6 and represents an end of separation-collapse scenario with round optics, an operational regime in which beam-beam effects are expected to be particularly pronounced. This setup corresponds to a beam energy of 7 TeV, alternating horizontal and vertical crossing angles across the interaction points. The optics feature a β^* of 1.1 m in IP1/5 and 1.5 m in IP2/8, with a half crossing angle of 250 µrad in IP1/5. A complete list of the simulation parameters used can be found in [12].

We perform a scan over the tune and strength of the Landau octupoles, focusing on a subset of the parameter space previously explored in [12], which exhibited the highest DA values. The tune Q_x is varied between 62.3150 and 62.3155, with $Q_y = Q_x - 2.0 + 0.005$. The octupole currents are varied between −300 and 0 A. The resulting DA, evaluated for 10^6 turns, is shown in Fig. 1 (top). The scan reveals a region of stability in the parameter space where the DA exceeds 10 σ, which we identify as suitable for further analysis. Within this stable region, we select three sets of parameters, labelled C1, C2 and C3, whose DA values as a function of number of turns, up to 2×10^6, are presented in Fig. 2. These configurations form the basis for the subsequent time-dependent studies.

* Work supported by the HL-LHC project.

ISBN: 978-3-95450-248-6 ISSN: 2673-5490 doi: 10.18429/JACoW-IPAC2025-WEPM061

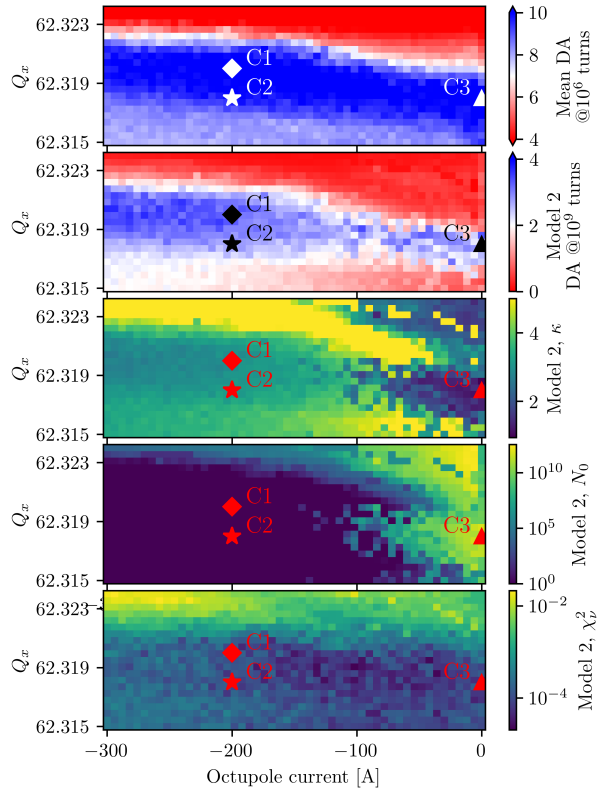

Figure 1: From top to bottom, DA as a function of tune and Landau octupole current, DA extrapolation via scaling law, κ and N_0 fitted values for each configuration, and achieved χ^2_ν. The three selected configurations are marked with dots.

Tracking simulations have been complemented by the exploration of DA extrapolation using a scaling law previously developed for static lattice conditions. We adopt "Model 2" from [11], defined as

$$\mathrm{DA}(N) = \rho_* \left(\frac{\kappa}{2e}\right)^{\kappa} \ln^{-\kappa}\left(\frac{N}{N_0}\right), \qquad (1)$$

where N is the number of turns considered, and ρ_*, κ, and N_0 are the free parameters. For each configuration, the parameters are determined by first performing a brute-force scan over a fixed interval, namely, $\rho_* \in [10^{-10}, 10^{10}]$, $\kappa \in [0.01, 5.00]$, and $N_0 \in [10^0, 10^6]$, followed by a local optimisation using gradient descent initialized from the best-scoring point of the scan. For numerical stability, we use the logarithm of the DA in the fitting procedure, and we also fit ρ_* and N_0 in logarithmic space.

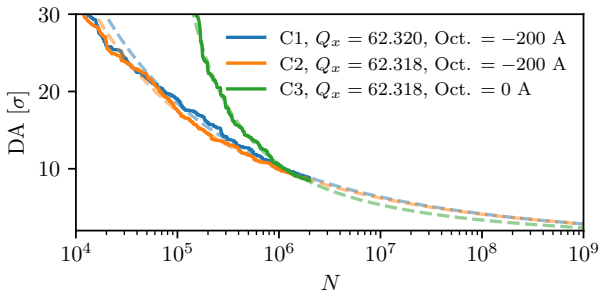

Figure 2: DA vs. N for the three selected configurations. Extrapolated DA at 10^9 turns is shown in dahsed lines.

The extrapolated DA at 10^9 turns, shown in Fig. 2, reveals a narrower and more selective region with relatively high DA compared to that at 10^6 turns. C3 shows the highest DA at early times, significantly outperforming C1 and C2 below 10^6 turns. At 10^6 turns, the values are closer (C1 = 11.06σ, C2 = 10.71σ, C3 = 11.80σ), but C3 then degrades more rapidly. By 2×10^6 turns, all configurations converge, and at 10^9 turns, C1 and C2 reach 2.86 σ, while C3 drops to 2.36 σ. This shows that high DA at an intermediate number of turns does not ensure better long-term stability, highlighting the need to consider asymptotic behaviour in performance assessments.

Furthermore, Fig. 1 highlights the emergence of two distinct fitting regimes: in some cases, such as C3, the fit converges to $\kappa < 2$ with finite N_0, while in others, $\kappa > 3$ and N_0 saturates at its lower bound of 1. This divergence and saturation behaviour, already observed in previous studies [11], is attributed to strong correlations among the model parameters. The presence of these two regimes suggests that, in some cases, octupole fields may trigger resonance overlap, which is not fully captured by the scaling law, because the underlying stability-time estimate from Nekhoroshev theorem does not consider this regime.

Setup of Time-Dependent Tracking

Starting from three parameter sets, we define the corresponding time-dependent lattice variations: one involving tune changes (C1 ⇄ C2), one involving octupole current changes (C2 ⇄ C3), and one combining both (C1 ⇄ C3). Considering each variation in both directions of change results in six distinct modification scenarios. Using the flexibility of Xsuite [14, 16], these variants can be implemented without affecting the performance of tracking simulations.

In this study, we focus on two representative types of time-dependent lattice alterations, for a total of twelve configurations: a sudden step-like change in the relevant settings at a specific time, and a gradual linear change applied in increments over fixed intervals. Each simulation includes 2×10^6 tracking turns, with the first 10^6 turns dedicated to the application of the time-dependent perturbation, and the remaining 10^6 turns used to evaluate its impact on the DA. For the step-like change, the perturbation is applied at turn 5×10^5, while for the gradual change, the perturbation is applied in increments of 10^4 turns, for a total of 100 increments over the span of the initial 10^6 turns.

NUMERICAL RESULTS

An overview of the DA observed for the twelve variations of the lattice is shown in Fig. 3. The DA scaling law has been applied to every configuration, with the resulting fitting parameters and χ^2_ν shown in Table 1. The extrapolated DA at 10^9 turns is also included. These configurations span a range of DA regimes, with C1 and C2 representing a relatively

ISBN: 978-3-95450-248-6 ISSN: 2673-5490 doi: 10.18429/JACoW-IPAC2025-WEPM061

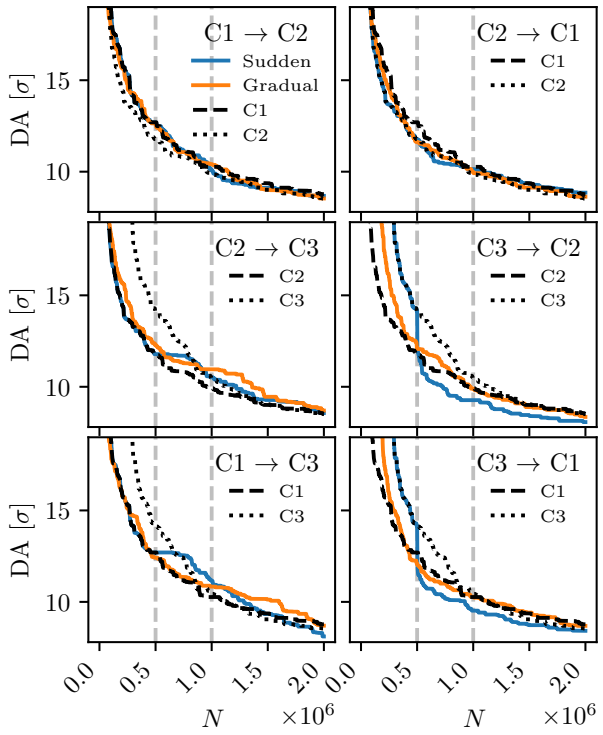

Figure 3: Overview of DA over N for the twelve time-dependent configurations. DA of initial and final static configurations are also shown for comparison by dashed and dotted lines, respectively.

stable condition and C3 an initially very stable condition, which then degrades rapidly.

The DA evolution curves show that sudden parameter changes between static configurations with strongly differing DA behaviour can trigger abrupt stability shifts, appearing as sharp drops or immediate improvements depending on the transition direction. For instance, in the C3 → C1 transition, the DA experiences a sudden drop at the 5×10^5 turn mark. In contrast, during the C1 → C3 transition, the DA remains stable immediately after the sudden change is applied, before gradually degrading and aligning with the DA trend of the C3 baseline. On the other hand, gradual parameter changes result in a smoother, more continuous evolution of the DA, avoiding abrupt transitions.

The extrapolated DA at 10^9 turns indicates that long-term stability is more influenced by the initial configuration than the final one. For instance, the transition C3 →1 yields a lower DA (2.60 σ) than the reverse case 1→C3 (2.93 σ), despite both involving the same endpoint configurations. A similar trend appears in C2→C3 (3.16 σ) versus C3→ C2 (2.31 σ). These asymmetries suggest that the system retains a memory of its starting condition, particularly when evolving from less stable configurations. This would imply that simply reaching a more stable configuration may not be sufficient to recover optimal long-term performance.

A consistent trend across almost all cases is that gradual transitions yield higher extrapolated DA values than sudden ones, indicating improved beam stability under smoother (adiabatic) parameter changes. For example, the C2 → C3 transition improves from 3.16 σ (sudden) to 3.23 σ (gradual), and C3 → C1 shows a remarkably larger gain from 2.60 σ to 4.41 σ, even surpassing the C1 baseline of 2.93 σ. This, combined with the higher χ^2_ν values observed in some sudden transitions, suggests that the DA scaling law may be less reliable for sudden changes.

Table 1: Fitting parameters and χ^2_ν of the DA scaling law obtained for all selected configurations and time-dependent variations (S stands for sudden change, G for gradual change). Measured DA at 2×10^6 turns (first entry) and extrapolated DA at 10^9 turns (second entry) are also shown. Uncertainty on the last digit is shown in parentheses.

Exp.	χ^2_ν $\times 10^{-4}$	κ	$\log_{10}\rho_*$	$\log_{10} N_0$	DA [σ] (Last / Ex.)
C1	1.2	3.2(2)	4.2(2)	0.0(4)	8.78/2.86
C2	0.4	3.07(7)	4.15(7)	0.00(7)	8.50/2.87
C3	0.8	1.44(2)	2.17(2)	4.36(2)	8.53/2.37
1→2, S	2.2	3.3(2)	4.3(2)	0.0(2)	8.68/2.71
1→2, G	1.8	3.2(2)	4.2(2)	0.00(4)	8.53/2.82
2→1, S	0.5	2.85(7)	3.99(7)	0.2(2)	8.85/3.10
2→1, G	0.6	3.10(9)	4.18(9)	0.0(2)	8.63/2.87
2→3, S	1.6	2.93(2)	4.08(2)	0.00(3)	8.56/3.16
2→3, G	1.7	2.93(2)	4.09(2)	0.0(2)	8.70/3.23
3→2, S	7.9	1.26(2)	1.98(2)	4.56(2)	8.07/2.31
3→2, G	0.9	0.725(4)	1.692(3)	4.787(3)	8.35/4.03
1→3, S	6.2	3.2(2)	4.2(2)	0.0(2)	8.10/2.93
1→3, G	1.4	2.93(2)	4.10(2)	0.0(2)	8.70/3.28
3→1, S	6.5	1.17(2)	1.95(2)	4.60(2)	8.42/2.60
3→1, G	0.9	0.663(4)	1.663(3)	4.82(3)	8.69/4.41

Apart from these specific cases, the scaling law fits generally show good agreement with the tracking data, with χ^2_ν below 2.0×10^{-4} in most cases, thus supporting the robustness of the extrapolation model. Higher fit residuals are observed in sudden transitions from C3 (e.g., C3 → C1, C3 → C2), where strong nonlinearity leads to low κ and large N_0, indicating slow DA decay. In contrast, stable configurations yield high κ and $N_0 \to 1$, reflecting rapid stabilisation.

CONCLUSIONS AND OUTLOOK

We studied the DA under time-dependent parameter changes in HL-LHC lattices using tracking and scaling-law extrapolation. Gradual transitions ensure stability, while long-term DA was mostly determined by the initial configuration, indicating a strong memory effect. Two distinct fit regimes were observed, possibly linked to octupole-induced resonances. Despite some reduced fit quality, the scaling law proved reliable in all cases. This work and its findings serve as a first exploratory step toward realistic time-dependent modelling, highlighting the complementary role of tracking and extrapolation. Future studies will extend the approach to include effects such as crossing angles and β^* levelling.

ISBN: 978-3-95450-248-6 ISSN: 2673-5490 doi: 10.18429/JACoW-IPAC2025-WEPM061

REFERENCES

[1] G. Apollinari *et al.*, "High-Luminosity Large Hadron Collider (HL–LHC)", CERN, Geneva, Rep. CERN-2017-007-M, 2017. doi:10.23731/CYRM-2017-004

[2] O. S. Brüning *et al.*, "LHC Design Report", CERN, Geneva, Rep. CERN-2004-003-V-1, 2004. doi:10.5170/CERN-2004-003-V-1

[3] H. Damerau *et al.*, "LHC Injectors Upgrade, Technical Design Report", CERN, Geneva, Switzerland, Rep., Dec. 2014. doi:10.17181/CERN.7NHR.6HGC

[4] S. Fartoukh, M. Solfaroli, J. C. De Portugal, A. Mereghetti, A. Poyet, and J. Wenninger, "Achromatic telescopic squeezing scheme and by-products: From concept to validation", *Phys. Rev. Accel. Beams*, vol. 24, no. 2, p. 021002, Feb. 2021. doi:10.1103/PhysRevAccelBeams.24.021002

[5] R. Calaga, E. Jensen, G. Burt, and A. Ratti, "Crab cavity development", in *The High Luminosity Large Hadron Collider*. World Scientific, 2015, pp. 137–156. doi:10.1142/9789814675475_0007

[6] E. Todesco and M. Giovannozzi, "Dynamic aperture estimates and phase-space distortions in nonlinear betatron motion", *Phys. Rev. E*, vol. 53, no. 4, pp. 4067–4076, Apr. 1996. doi:10.1103/PhysRevE.53.4067

[7] M. Giovannozzi, "A proposed scaling law for intensity evolution in hadron storage rings based on dynamic aperture variation with time", *Phys. Rev. Spec. Top. Accel Beams*, vol. 15, no. 2, p. 024001, Feb. 2012. doi:10.1103/PhysRevSTAB.15.024001

[8] J. Barranco Garcia and T. Pieloni, "Global compensation of long-range beam-beam effects with octupole magnets: dynamic aperture simulations for the HL-LHC case and possible usage in LHC and FCC", CERN, Geneva, Switzerland, Rep. CERN-ACC-NOTE-2017-0036, 2017. https://cds.cern.ch/record/2263347

[9] K. Skoufaris *et al.*, "Numerical optimization of DC wire parameters for mitigation of the long range beam-beam interactions in High Luminosity Large Hadron Collider", *Phys. Rev. Accel. Beams*, vol. 24, no. 7, p. 074001, Jul. 2021. doi:10.1103/PhysRevAccelBeams.24.074001

[10] M. Giovannozzi, W. Scandale, and E. Todesco, "Dynamic aperture extrapolation in presence of tune modulation", *Phys. Rev. E*, vol. 57, no. 3, p. 3432, Mar. 1998. doi:10.1103/PhysRevE.57.3432

[11] A. Bazzani, M. Giovannozzi, E. H. Maclean, C. E. Montanari, F. F. Van der Veken, and W. Van Goethem, "Advances on the modeling of the time evolution of dynamic aperture of hadron circular accelerators", *Phys. Rev. Accel. Beams*, vol. 22, no. 10, p. 104003, Oct. 2019. doi:10.1103/PhysRevAccelBeams.22.104003

[12] C. Droin *et al.*, "Status of beam-beam studies for the high-luminosity LHC", in *Proc. IPAC'24*, Nashville, TN, USA, 2024, pp. 3213–3216. doi:10.18429/JACoW-IPAC2024-THPC77

[13] Xsuite documentation, 2023. http://xsuite.web.cern.ch

[14] G. Iadarola *et al.*, "Xsuite: an integrated beam physics simulation framework", in *Proc. IPAC'24*, Nashville, TN, USA, pp. 2623–2626, Jul. 2024. doi:10.18429/JACoW-IPAC2024-WEPR56

[15] W. Herr and T. Pieloni, "Beam-beam effects", in *CAS - CERN Accelerator School: Advanced Accelerator Physics*, pp. 431–459, 2016. doi:10.5170/CERN-2014-009.431

[16] *Xsuite physics reference manual*, 2022. https://github.com/xsuite/xsuite/blob/main/docs/physics_manual/physics_man.pdf